

CHAPTER 104

Generation of Infragravity Waves

A.R. Van Dongeren, I.A. Svendsen and F.E. Sancho¹

ABSTRACT: In this paper the depth-integrated, short wave-averaged nearshore circulation model SHORECIRC is used to study the generation of infragravity waves due to normally incident short wave groups on a plane beach. After linear separation of the incident and reflected long waves, it is shown that the incoming long wave shoals faster than Green's Law predicts for free waves. This indicates that energy is transferred from the short wave groups to the long wave. However, it does not shoal as quickly as Longuet-Higgins & Stewart's (1962) steady state theory for bound waves suggests. The outgoing long wave deshoals according to Green's Law but it is shown that energy is traded back and forth with the incoming short wave groups. Different shoaling and deshoaling curves can be found for different parameter choices. The work term in the long wave energy equation is used to explain these differences and ratio of the number of short wave groups to the surf zone width is confirmed to be an important parameter. As a consequence, the energy of the outgoing long wave can be larger or smaller than that of the incoming long wave, depending on the value of that parameter. Finally, the nonlinear version of the model shows the importance of the mean set-up on the generation of long waves, in particular very close to the shoreline.

INTRODUCTION

It is well-known that a forced long wave propagates with short wave groups at the group speed (Longuet-Higgins & Stewart, 1962) [LHS62 in the remainder]. When these groups propagate onto a beach, the short waves shoal and break. In the shoaling process the incoming, bound long wave gains energy and is released from the groups. The incoming long wave propagates shoreward, interacts with the breaking process, eventually reflects off the beach and propagates seaward as a free wave. The principle of this process is generally agreed upon, but the precise mechanisms by which energy is transferred to the long (or infragravity) waves are not.

For the case of normally incident waves, two different infragravity wave generation mechanisms have been proposed for the interaction with the breaking. Symonds *et al.* (1982) assumed that the groupiness which existed outside the

¹Center for Applied Coastal Research, Ocean Engineering Lab, University of Delaware, Newark, DE 19716, USA. Correspondence e-mail: apper@coastal.udel.edu

breaker zone is destroyed by the breaking and that the short waves inside the surf zone will decay with a saturated wave height. This implies a time-varying break point which generates long waves while no long wave generation takes place inside the surf zone.

Schäffer & Svendsen (1988) [SS88] examined the other extreme where all short waves regardless of their height are assumed to break at a fixed break point. This means that the groupiness outside the surf zone is transmitted into the surf zone where long wave generation can take place.

It is likely that neither mechanism is exclusively responsible for long wave generation but that it is due to a combination of both effects. Therefore Schäffer (1993) [S93] merged the two extreme mechanisms into one hybrid analytical solution and showed the effects of parameter variations.

Some field studies suggest that there is more energy in the free (outgoing or trapped) waves than in the incoming bound waves (Munk, 1949; Tucker, 1950; Elgar *et al.*, 1992; Herbers *et al.*, 1995 to name a few). This indicates that in the nearshore region energy has been transferred from the short waves to the long waves. However, other observations (Guza & Thornton, 1985; Kostense, 1984) show that the energies of the in- and outgoing long waves are about equal, which means that no net long wave energy was gained.

In this paper the nearshore circulation model SHORECIRC (Van Dongeren *et al.*, 1994) is applied to study the generation of infragravity waves on a plane beach with normally incident short wave groups. In the next section, the general governing equations of nearshore circulation are stated. Then, the linearized version of the model is used to study the growth of the amplitude of the incoming and outgoing long waves for different parameter choices. The linear long wave energy equation is used to explain the characteristics of the shoaling and deshoaling curves. It is shown that net energy can either be gained or lost depending on the values of certain parameters. Finally, the nonlinear version of the model reveals the importance of the nonlinear terms, in particular the mean set-up of the surface elevation.

GOVERNING EQUATIONS

The depth-integrated, time-averaged mass and momentum equations read (Van Dongeren *et al.*, 1994; Svendsen & Putrevu, 1996):

$$\frac{\partial \bar{\zeta}}{\partial t} + \frac{\partial}{\partial x_\alpha} \left(\int_{-h_0}^{\bar{\zeta}} V_\alpha dz + Q_{w\alpha} \right) = 0 \quad (1)$$

$$\begin{aligned} \frac{\partial \bar{Q}_\beta}{\partial t} + \frac{\partial}{\partial x_\alpha} \left(\frac{\bar{Q}_\alpha \bar{Q}_\beta}{h} \right) + \frac{\partial}{\partial x_\alpha} \int_{-h_0}^{\bar{\zeta}} V_{1\alpha} V_{1\beta} dz + \frac{\partial}{\partial x_\alpha} \int_{\zeta t}^{\bar{\zeta}} \overline{u_{w\alpha} V_{1\beta} + u_{w\beta} V_{1\alpha}} dz \\ + g(h_0 + \bar{\zeta}) \frac{\partial \bar{\zeta}}{\partial x_\beta} + \frac{1}{\rho} \frac{\partial}{\partial x_\alpha} \left(S_{\alpha\beta} - \int_{-h_0}^{\bar{\zeta}} \tau_{\alpha\beta} dz \right) - \frac{\tau_\beta^S}{\rho} + \frac{\tau_\beta^B}{\rho} = 0 \end{aligned} \quad (2)$$

where the total current has been split into depth uniform and depth varying components:

$$V_\alpha = \frac{\bar{Q}_\alpha}{h_0 + \bar{\zeta}} + V_{1\alpha}(x, y, z, t) \quad (3)$$

which implies

$$\int_{h_o}^{\bar{\zeta}} V_{1\alpha} dz = -Q_{w\alpha} \quad (4)$$

It turns out that in this formulation the radiation stress $S_{\alpha\beta}$ is defined as by Mei (1983). For a discussion of the details see Svendsen & Putrevu (1996).

In (1) and (2), V_α and $\bar{\zeta}$ represent the horizontal current velocity and the mean surface elevation, respectively. u_w is the short wave velocity defined so that $\bar{u}_w = 0$ below through level, \bar{Q}_α represents the total volume flux and $Q_{w\alpha}$ is the volume flux due to the short wave motion. ζ_t is the elevation of the wave trough, $\tau_{\alpha\beta}$ is the Reynolds stress, h_o is the still water depth, while τ_β^S and τ_β^B represent the surface and the bottom shear stress, respectively. The overbar denotes short wave averaging and the subscripts α and β denote the directions in a Cartesian coordinate system. Fig. 1 shows the definitions.

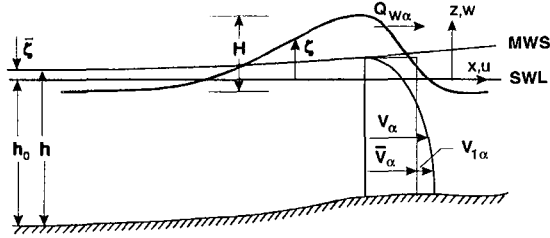


Figure 1: Definition sketch.

For the present purpose we will consider depth-uniform long waves in the shore-normal x -direction, which reduces the set of equations to:

$$\frac{\partial \bar{\zeta}}{\partial t} + \frac{\partial \bar{Q}}{\partial x} = 0 \quad (5)$$

$$\frac{\partial \bar{Q}}{\partial t} + \frac{\partial}{\partial x} \left(\frac{\bar{Q}^2}{h} \right) + g(h_o + \bar{\zeta}) \frac{\partial \bar{\zeta}}{\partial x} + \frac{1}{\rho} \frac{\partial S_{xx}}{\partial x} + \frac{\tau_x^B}{\rho} = 0 \quad (6)$$

These equations correspond to the forced nonlinear shallow water equations where the radiation stress gradient provides the forcing on the long waves. The equations are solved by finite differences using a second-order predictor-corrector method for time and horizontal space on a fixed rectangular grid. On the seaward side we specify an absorbing-generating boundary condition as derived by Van Dongeren & Svendsen (1996). In the linear version of the model a no-flux boundary condition is specified at the still water line while in the nonlinear version a moving shoreline condition is used (Van Dongeren *et al.*, 1995).

LINEAR ANALYSIS

The simplest possible case to analyze is a plane beach with a shelf and forcing generated by a bichromatic short wave group while using the linearized version of the model. This case provides valuable insights into the long wave generation mechanisms.

Following SS88 and S93 we can write the radiation stress forcing as:

$$S_{xx} = \frac{1}{2} \rho g \left(2n - \frac{1}{2} \right) \begin{cases} a_1^2 \left(1 + 2\delta \cos \left(f \frac{\Delta\omega}{c_g} dx - \Delta\omega t \right) \right), & h \geq h_b \\ \gamma^2 h_o^2 \left(1 + 2\delta(1 - \kappa) \cos \left(f \frac{\Delta\omega}{c_g} dx - \Delta\omega t \right) \right), & h \leq h_b \end{cases} \quad (7)$$

where κ is the parameter controlling the generation mechanism: $\kappa = 0$ corresponds to the case of a fixed break point, while $\kappa = 1$ represents the time-varying break point case. $n = c_g/c$ where c_g is the group speed. a_1 is the amplitude of the primary short wave in the group while the groupiness $\delta = a_2/a_1$ is the ratio of the amplitude of the secondary wave and the primary wave. $\Delta\omega = \omega_1 - \omega_2$ is the difference frequency between the two short waves which is also the long wave frequency. $\gamma = 2a_1/h$ is the saturated wave height over water depth ratio. h_b is the breaking depth. It is important to notice that the forcing consists of a steady part - which causes a steady set-up - and a time-varying part which forces a long wave. In our analysis we are only interested in the latter and in the rest of the paper we show only the time varying part of the solution.

It is assumed that the shelf is wide enough so that at the toe of the beach the incoming long wave corresponds to the equilibrium bound long wave for the flat shelf:

$$\bar{\zeta}_i = -\frac{1}{\rho} \frac{S_{xx}^{(1)}}{g h_s - c_{gs}^2} \quad (8)$$

where the subscript $_s$ corresponds to conditions on the shelf and $S_{xx}^{(1)}$ is the time-varying part of the forcing of (7). The outgoing wave is absorbed using the absorbing-generating boundary condition referenced above.

Case 1: fixed breakpoint

The first case considered is that of a fixed breakpoint ($\kappa = 0$) corresponding to the mechanism proposed by SS88. In the example studied, the following parameter values are used: forcing frequency $\Delta\omega = 0.422 \text{ s}^{-1}$, primary wave amplitude $a_{1,s} = 0.4415 \text{ m}$ on the shelf, groupiness $\delta = 0.1$, saturated breaking parameter $\gamma = 0.7$, beach slope $h_x = 1/30$ and shelf depth $h_s = 3 \text{ m}$.

The solid line in Fig. 2a shows the envelope of the long wave versus the depth, nondimensionalized by the shelf depth. The surface elevations are normalized by $a_{1,s}^2 \delta / h_s$, so that the incoming bound long wave of (8) is $O(1)$ at the offshore boundary. In the Figure, the still water line is on the left-hand side while the toe of the beach is on the right-hand side. Notice the agreement of the model with the dashed line which corresponds to the analytical solution by SS88. The break point is located at $h/h_s = 0.45$ and is indicated in the Figure.

The long wave can be separated into an incoming and an outgoing long wave

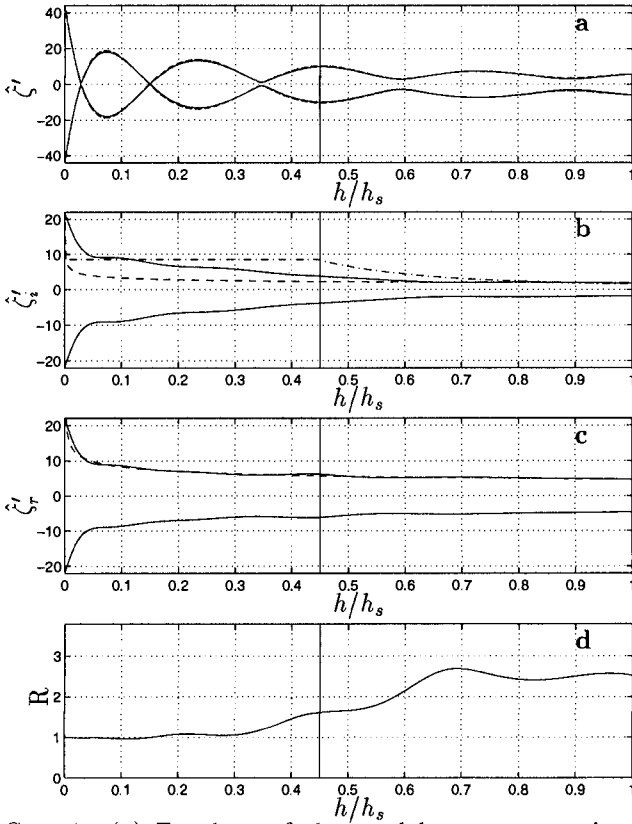


Figure 2: Case 1: (a) Envelope of the total long wave motion vs. depth : present model (—) and analytical solution (- -); (b) Envelope of the incoming long wave: present model (—), Green's Law (- -) and LHS62's steady state solution (-·-); (c) Envelope of the outgoing long wave: present model (—) and Green's Law (- -); (d) Reflection coefficient.

using linear superposition of the surface elevation and the flux

$$\bar{\zeta} = \bar{\zeta} + \bar{\zeta}_i + \bar{\zeta}_r \quad \text{and} \quad \bar{Q} = \bar{Q}_i + \bar{Q}_r \quad (9)$$

where $\bar{\zeta}$ is the steady set-up, subscript i denotes the incoming wave and subscript r denotes the outgoing wave. Also, we know the following relationships between the surface elevation and the flux of the incoming and outgoing wave, respectively:

$$\bar{Q}_i = c_g \bar{\zeta}_i \quad \text{and} \quad \bar{Q}_r = -\sqrt{g h_o} \bar{\zeta}_r \quad (10)$$

which implies that the incoming wave essentially propagates with group speed c_g and the free outgoing wave propagates with the shallow water wave speed.

This is confirmed by the computations. Solving for $\bar{\zeta}_i$ and $\bar{\zeta}_r$ from these four equations yields

$$\bar{\zeta}_i = \frac{\sqrt{g h_o} (\bar{\zeta} - \bar{\zeta}) + \bar{Q}}{c_g + \sqrt{g h_o}} \quad \text{and} \quad \bar{\zeta}_r = \frac{c_g (\bar{\zeta} - \bar{\zeta}) - \bar{Q}}{c_g + \sqrt{g h_o}} \quad (11)$$

The solid line in Fig. 2b shows the envelope of the *incoming* long wave. Note that the long wave shoals faster than as predicted by Green's Law ($\hat{\zeta} \propto h^{-1/4}$, the dashed line), which means that energy must have been transferred to the long wave. Also shown is the shoaling curve according to LHS62's steady state theory, Eq. (8) (the dash-dotted line, $\hat{\zeta} \propto h^{-5/2}$ outside the surf zone), which grows much faster than the actual wave. This indicates that on a sloping beach the bound long wave does not have "time" to attain local equilibrium but that it depends on its history. Therefore, on the slope the forced long wave does not increase with depth as $h^{-5/2}$ as is assumed in the analysis of field data in some papers (e.g., Elgar *et al.*, 1992; Herbers *et al.*, 1995).

In Fig. 2c the outgoing long wave (solid line) closely follows Green's Law (dashed line) which indicates that this wave is a free long wave. There are some oscillations noticeable around the dashed line because energy is traded back and forth with the incoming short wave group, as will be explained below.

Figure 2d shows the ratio of the amplitude of the outgoing wave and the incoming wave (the "reflection coefficient"). This ratio is by definition equal to unity at the shore. For the chosen parameter values, the ratio is larger than unity everywhere else, meaning that there is more energy in the outgoing wave than in the incoming wave, which indicates that energy has been transferred from the short waves to the long waves.

As a tool to study this energy transfer in more detail we can use the linear long wave energy equation

$$\frac{\partial E}{\partial t} + \frac{\partial E_f}{\partial x} + \frac{\bar{Q}}{h_o} \frac{\partial S_{xx}}{\partial x} = 0 \quad (12)$$

where E is the long wave energy, $E_f = \rho g \bar{\zeta} \bar{Q}$ is the energy flux and the third term represents the work the short waves do on the long wave through the radiation stress. Averaging over the IG-wave period (denoted by the double overbar) eliminates the temporal variation and yields a balance between the energy flux and the work

$$\frac{\partial \overline{\overline{E_f}}}{\partial x} + \frac{\overline{\overline{Q}}}{h_o} \frac{\partial \overline{\overline{S_{xx}}}}{\partial x} = 0 \quad (13)$$

The two terms can be each split into an incoming and outgoing part

$$\frac{\partial \overline{\overline{E_{f,i}}}}{\partial x} + \frac{\partial \overline{\overline{E_{f,r}}}}{\partial x} + \frac{\overline{\overline{Q_i}}}{h_o} \frac{\partial \overline{\overline{S_{xx}}}}{\partial x} + \frac{\overline{\overline{Q_r}}}{h_o} \frac{\partial \overline{\overline{S_{xx}}}}{\partial x} = 0 \quad (14)$$

Figure 3a shows the balance between the energy flux term (dashed line) and the work term (solid line) in (13) across the domain for the same parameter

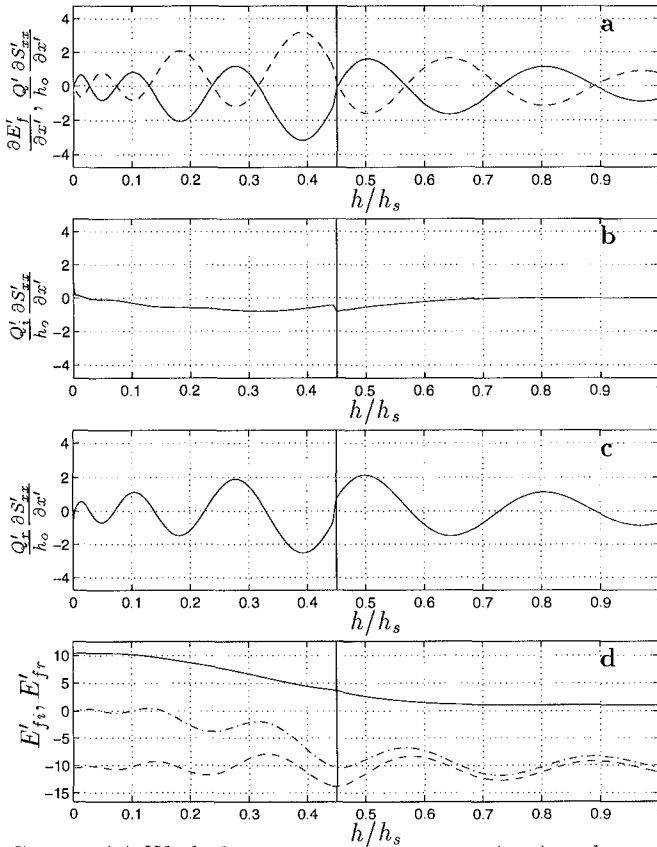


Figure 3: Case 1: (a) Work done on total long wave (—) and energy flux (- -); (b) Work on incoming long wave; (c) Work on outgoing long wave; (d) Energy flux of incoming wave (—), energy flux of outgoing wave (- -), and energy flux of total long wave (- .).

values as in Fig. 2. Both terms are normalized by $\rho g \sqrt{gh_s} \delta^2 a_{1,s}^4 / h_s^3$. Figure 3b shows the work done on the incoming wave which is the third term in (14). It is negative across the whole domain, which means that energy flux is gained. This is consistent with the finding of Fig. 2 that the incoming long wave increases faster in amplitude than a free long wave. Conversely, Fig. 3c reveals that the work done by the short waves on the outgoing long wave oscillates around zero, which means that energy is traded back and forth but that over the whole domain the long wave loses or gains very little energy. It essentially deshoals as a free long wave as was already seen in Fig. 2c.

In Fig. 3d the energy fluxes of the incoming, the outgoing and the total long wave motion are shown, normalized by $\rho g \sqrt{gh_s} \delta^2 a_{1,s}^4 / h_s^2$. Notice that the incoming wave already gains about 30% of energy flux seaward of the break point. The incoming long wave reaches its maximum energy flux at the shore-

line where it is fully reflected. The outgoing wave shows an oscillating energy flux. The total energy flux therefore becomes increasingly negative seawards as a consequence of the net transfer of energy from the short waves to the long wave.

Case 2a: moving breakpoint

The second case considered is that of a moving breakpoint ($\kappa = 1$) corresponding to the mechanism proposed by Symonds *et al.* (1982). The same parameter values as in case 1 are used.

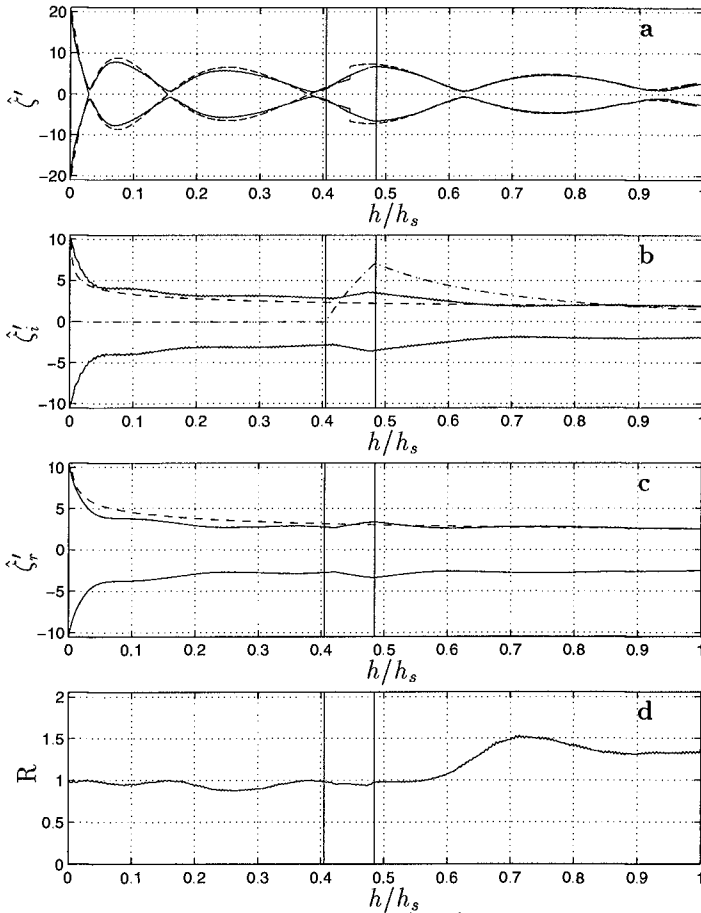


Figure 4: Case 2a: labels as Fig. 2. The breaking region is indicated by the vertical lines.

Figure 4a shows the comparison of the long wave envelope as predicted by the model and the analytical solution by S93. The differences are due to the fact that in the analytical solution the breaking region (ranging from $0.41 \leq h/h_s \leq 0.48$) is contracted into a point at $h/h_s = 0.45$ whereas the model is capable of reproducing the breaking region itself.

Up to the point where breaking starts, the incoming long wave in Fig. 4b gains energy flux as before. Over the breaking region, however, the energy flux is now decreasing, a feature which is investigated in more detail below. Inside the surf zone ($h/h_s \leq 0.41$) a standing long wave occurs due to the absence of forcing in that region, see Figs. 4b and c. Figure 4c shows that outside the surf zone the long wave again deshoals according to Green's Law.

Finally, the ratio of the amplitudes of the outgoing wave and the incoming wave is shown in Fig. 4d. Though the long wave energy is reduced through the breaking region the amplitude of the outgoing wave is still about equal to or larger than that of the incoming wave.

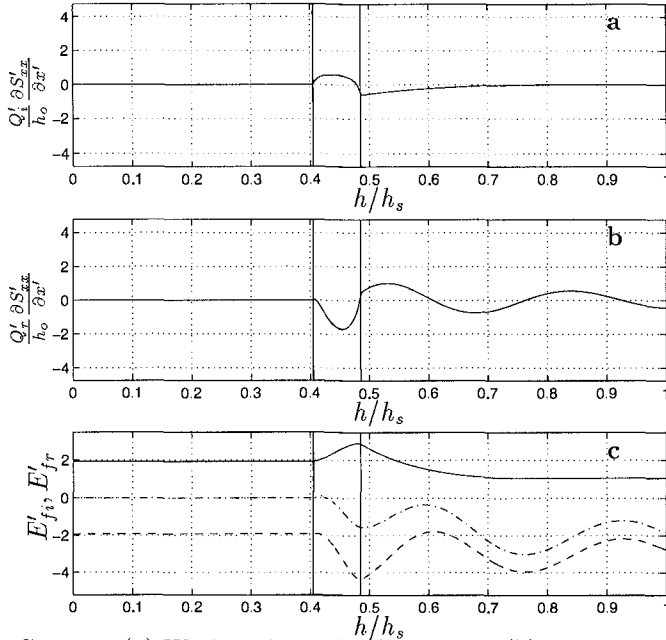


Figure 5: Case 2a: (a) Work on incoming long wave; (b) Work on outgoing long wave; (c) Energy flux of incoming wave (—), energy flux of outgoing wave (---) and energy flux of total long wave (-.-); The breaking region is indicated by the vertical lines.

This is further illustrated by the direct analysis of the energy transfer in Fig. 5. Panel (a) shows that in case 2a the work done on the incoming wave by the short waves in the breaking region itself is positive, which indicates an energy flux loss. This is consistent with the loss of amplitude shown in Fig. 4b. Inside the surf zone no forcing occurs, so the work is zero.

Fig. 5b shows that through the breaking region the work done on the outgoing wave is negative so that energy flux is *gained* (in magnitude) when the wave propagates out. Seaward of breaking the work is oscillating around zero as in case 1. The according energy fluxes of the incoming, outgoing and total wave are plotted in Fig. 5c.

Case 2b: moving breakpoint with halved forcing frequency

The results of case 2a are valid only for the chosen set of parameters. It turns out that a profound change occurs when the forcing frequency or the beach slope are varied. Either of these parameters control the number of wave groups in the surf zone, which is an important parameter, as will be shown below.

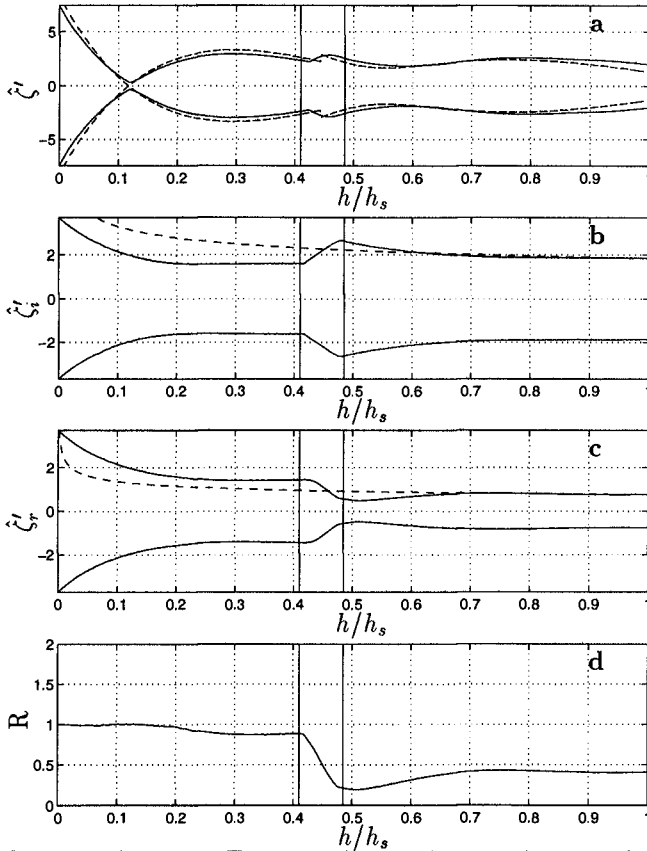


Figure 6: Case 2b: labels as Fig. 2. The breaking region is indicated by the vertical lines.

The conditions of case 2a are repeated except that the forcing frequency is halved, $\Delta\omega = 0.211 \text{ s}^{-1}$. Again the deviation between the model and the slightly simpler analytical solution is negligible (Fig. 6a). Fig. 6b shows that the amplitude of the incoming wave increases outside of the breaking region and decreases in the breaking region itself, similar to the previous case. Inside the surf zone forcing is absent and a standing wave occurs, see Figs. 6b and c. In this case, however, the outgoing long wave *loses* amplitude when propagating out through the breaking region (Fig. 6c). This results in a reflection coefficient less than unity outside the surf zone, i.e. the long waves have *lost* energy in the breaking process (Fig. 6d).

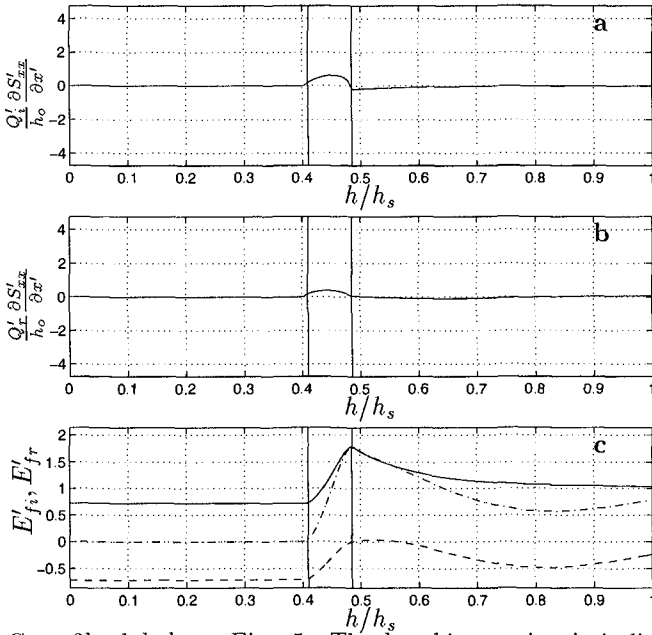


Figure 7: Case 2b: labels as Fig. 5. The breaking region is indicated by the vertical lines.

Analysis of the energy transfer using the terms in (14) confirms this result. Figure 7a is similar to Fig. 5a, but Fig. 7b shows that contrary to the previous case the work the short waves do on the outgoing long wave is now positive, which means that the energy flux decreases in magnitude as the long wave propagates out through the breaking region.

The reason for this different behavior is the phase difference between the short wave groups and the incoming and outgoing long waves. As the short waves propagate onto the beach, the phase shift between the associated incoming long wave and the groups grows from 0.5π to about 0.6π . This phase shift causes the work (which is the time-averaged product of the radiation stress gradient and the incoming long wave) to be negative so energy is transferred to the long waves. In the breaking region the forcing is varying in time (when the short waves in the group are smaller and break closer to shore) or constant (when the waves are larger and break further offshore). This causes the long wave-averaged work done on the incoming long wave to be positive in the breaking region. This behavior is independent of the period of the incoming wave groups.

With the destruction of the wave groups by the varying break point, the long wave is released in the breaking region and propagates shoreward as a free wave, where it is reflected and propagates seaward. The sign of the work that the short waves do on the outgoing wave is then dependent on the relative phase between them, which is a function of the time it takes the long wave to propagate through the surf zone and back. For a plane beach this time lag can be calculated as

twice the propagation time from the shore to the mean break point h_b :

$$\Delta T = 2 \int_0^{h_b} \frac{dh}{h_x \sqrt{gh}} = \frac{4}{h_x} \sqrt{\frac{h_b}{g}} \quad (15)$$

where $\Delta T = 44.5$ s in the cases considered here. In case 2a the ratio of the time lag ΔT to the group period $T_g = 2\pi/\Delta\omega$ is

$$\frac{\Delta T}{T_g} = \frac{2}{h_x} \sqrt{\frac{2a_b}{\gamma g}} \frac{\Delta\omega}{\pi} = 3 \quad (16)$$

This integer value means that the outgoing long wave is "in phase" with the incoming long wave in the breaking region (which is short relative to the long wave length). Because these waves propagate in opposite directions, the signs of the work terms are opposite as well. In case 2b the ratio $\Delta T/T_g$ is 1.5, which means the incoming and outgoing waves are in "anti-phase", which causes the work on the incoming and outgoing waves to have the same sign. The ratio $\Delta T/T_g$ essentially specifies the number of wave groups in the surf zone. As can be seen from (16) it depends on the forcing frequency, the beach slope and on the short wave amplitude at breaking. Instead of changing the forcing frequency, an equivalent variation of the beach slope would yield the same result.

This ratio is equivalent to the parameter \mathcal{X} which was already found by Symonds et al. (1982) and the slope parameter $S_b = h_x L_b/h_b$ used by SS88 where L_b is the length of the surf zone and h_b is the depth at breaking. Rewriting those parameters yields

$$\mathcal{X} \equiv \frac{\Delta\omega^2 h_b}{g h_x^2} = \frac{\pi^2}{4} \left(\frac{\Delta T}{T_g} \right)^2 = 4\pi^2 S_b^{-2} \quad (17)$$

IMPORTANCE OF NONLINEAR TERMS

To investigate the importance of nonlinearities on the results, the model is rerun with the parameters of case 2a but now using the nonlinear Equations (5) and (6). In this case it is impossible to linearly separate the incoming and outgoing long waves. Therefore, we will examine the terms in the nonlinear long wave equation, averaged over the IG-wave period

$$\frac{\partial}{\partial x} \overline{\left(\frac{1}{2} \rho \frac{Q^3}{h^2} + \rho g \zeta Q \right)} + \frac{\overline{Q}}{h} \frac{\partial \overline{S_{xx}}}{\partial x} + \overline{U \tau_{b,x}} = 0 \quad (18)$$

which is the nonlinear extension of (13). The work that the bottom friction is small and is neglected in the following. The energy flux and the work balance each other, as can be seen in Fig. 8a. It turns out that for the particular set of parameter values used here the same case run with the linearized equations (Fig. 8b) shows a change of sign of the terms. This is due to the fact that in the nonlinear version of the model the travel time ΔT is dependent on the still water depth h_o as well as the set-up $\bar{\zeta}$. In short, the set-up effectively changes the beach slope in the surf zone experienced by the long waves. Artificially including the mean set-up $\bar{\zeta}$ in the linear model reverses the sign of the terms, see Fig. 8c. In fact, it can be seen that Figs. 8a and c agree well, which indicates that the mean set-up is the most important nonlinear term.

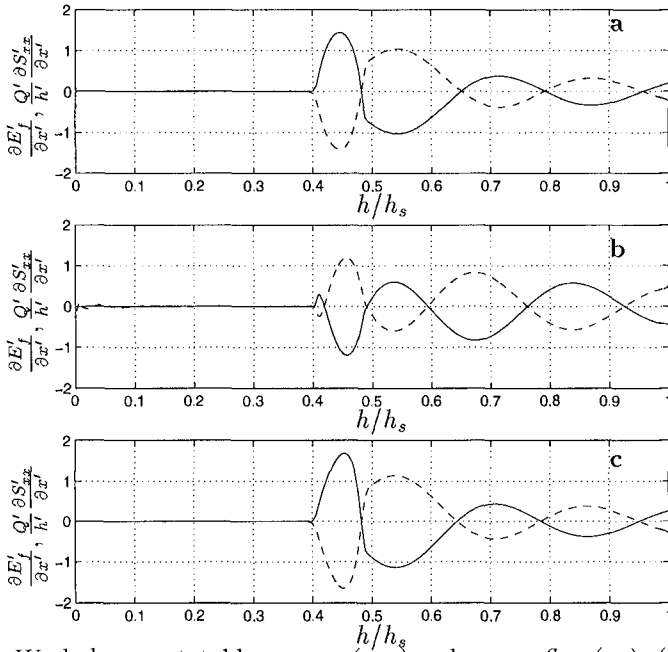


Figure 8: Work done on total long wave (—) and energy flux (- -): (a) Nonlinear version; (b) Linear version; (c) Linear version with mean set-up included in the depth.

CONCLUSIONS

The SHORECIRC model has been used to study infragravity wave generation. In the linear version of the model, the incoming and outgoing long waves can be separated. As expected, the incoming long wave already gains energy flux outside the surf zone due to the changing forcing but not nearly as fast as the local value of the LHS62 steady state theory for bound waves suggests. In the case of a fixed break point the energy flux gain continues inside surf zone, whereas in the case of a moving break point, it is found that the incoming wave loses energy flux in the varying break point region.

In the case of a fixed break point the outgoing long wave is seen to exchange energy flux with the short waves with very little net gain over the domain, so that it essentially deshoals according to Green’s Law. When the breakpoint is allowed to move, however, the outgoing wave either gains or loses flux depending on the phase between the short wave forcing and the outgoing wave. This gain or loss is dependent on a parameter which represents the number of wave groups in the surf zone. This result may explain the variation in the ratio of outgoing to ingoing wave energy found in field data.

Extending the model to include the nonlinear terms shows the importance of the steady set-up over the other nonlinear terms.

ACKNOWLEDGMENTS

Dr. H.A. Schäffer is gratefully acknowledged for making available his surf-beat computer code. This work is a result of research sponsored by NOAA Office of Sea Grant, Department of Commerce, under Award No. NA 56 RG 0147 (Project No. R/OE-17), by the U.S. Army Research Office, University Research Initiative under Contract No. DAAL03-92-G-0116 and Office of Naval Research (contract no. N00014-95-1-0075). The U.S. Government is authorized to produce and distribute reprints for government purposes notwithstanding any copyright notation that may appear herein.

REFERENCES

- Elgar, S., T.H.C. Herbers, M. Okihiro, J. Oltman-Shay and R. T. Guza (1992). Observations of infragravity waves. *Journal of Geophysical Research*, 97, pp. 15,573-15,577.
- Guza, R.T. and E.B. Thornton (1985). Observations of surf beat. *Journal of Geophysical Research*, 90, C2, pp. 3161-3171.
- Herbers, T.H.C., S. Elgar, R.T. Guza and W.C. O'Reilly (1995). Infragravity-Frequency (0.005-0.05 Hz) motions on the shelf. Part II: Free waves. *J. Phys. Oceanogr.*, 25, pp. 1063-1079.
- Kostense, J.K. (1984). Measurements of surf beat and set-down beneath wave groups. *Proc. of the 19th ICCE*, pp. 724-740.
- Longuet-Higgins, M.S. and R.W. Stewart (1962). Radiation stress and mass transport in gravity waves with application to 'surf-beats'. *J. of Fluid Mech.*, 8, pp. 565-583.
- Mei, C.C. (1983). The applied dynamics of ocean surface waves. John Wiley and Sons, New York, 740 pp.
- Munk, W.H. (1949). The solitary wave theory and its application to surf problems. *Annals of the New York Academy of Sciences*, 51, pp. 376-424.
- Schäffer, H.A. (1993). Infragravity waves induced by short-wave groups. *J. Fluid Mech.*, 247, pp. 551-588.
- Schäffer, H.A. and I.A. Svendsen (1988). Surf beat generation on a mild slope beach. *Proc. of the 21st ICCE*, pp. 1058-1072.
- Svendsen, I.A. and U. Putrevu (1996). Surf zone hydrodynamics. In *Advances in Coastal and Ocean Engineering*, Vol. 2, World Scientific Publ., pp. 1-78.
- Symonds, G., D.A. Huntley and A.J. Bowen (1982). Two dimensional surf-beat: Long wave generation by a time-varying break point. *J. of Geoph. Res.*, 87, C1, pp. 492-498.
- Tucker, M.J. (1950). Surf beats: sea waves of 1 to 5 minute period. *Proceedings of the Royal Society of London, A*, 202, pp. 565-573.
- Van Dongeren, A.R., F.E. Sancho, I.A. Svendsen and U. Putrevu (1994). SHORECIRC: A quasi 3-D nearshore model. *Proc. of the 24th ICCE*, pp. 2741-2754.
- Van Dongeren, A.R., I.A. Svendsen and F.E. Sancho (1995). Application of the Q-3D SHORECIRC model to surfbeat. *Proc. Coastal Dynamics*, pp. 233-244.
- Van Dongeren, A.R. and I.A. Svendsen (1996). An absorbing-generating boundary condition for shallow water models. Submitted to *J. of Wat., Port, Coastal and Ocean Eng.*